Feasibility of additive manufacturing processes for lunar soil simulants

Danijela Stupar, Grégoire Chabrol, Abdoul Razak, Sylvain Lecler, Alexandre Tessier, Thierry Cutard, Jocelyne Miehe-Brendle

Ignjatović Stupar, D., Chabrol, G. R., Baraze, A. R. I., Lecler S., Tessier, A., Cutard, T., Brendle, J.

FEASIBILITY OF ADDITIVE MANUFACTURING PROCESSES FOR LUNAR SOIL SIMULANTS

Abstract: *Combination of In-situ Resource Utilization (ISRU) and on-site Additive Manufacturing (AM) is one of the "outer space applied technologies" candidates where free shape fabrication from micro (e.g., tools) to mega scale (e.g. lunar habitats) will allow in coming future to settle the Moon or potentially other celestial bodies. Within this research, Selected Laser Melting (SLM) of lunar soil (regolith) simulants (LHS-1 LMS-1 and JSC-2A) using a continuous wave 100 W 1090 nm fiber laser was applied. The resulting samples were mechanically and optically characterized. A numerical multiphysics model was developed to understand the heat transfer and optimize the SLM process. Results obtained are in good agreement with the numerical model. The physical and chemical characteristics of the various materials (granulometry, density, composition, and thermal properties) have a strong impact on the AM parameters.*

1. INTRODUCTION

The lunar regolith is a dust like material that is derived from the degradation of the underlying rocks by the joint action of the impact of meteorites and solar winds on the surface of the Moon [1].

Characterization of lunar soil was done through samples collected during the Apollo and Luna missions. Having real material in hands and experiences gained by astronauts, researchers came with much clearer conclusions on how regolith, the main lunar soil material, behaves under different conditions, such as lack of atmosphere, low gravity, and extreme temperatures. The quantity of returned regolith was insufficient to be used worldwide as a test material in the development of new technological solution for future lunar settlement. One of the solutions was to create simulant materials which will be terrestrially exploited or artificially made to replace the original regolith. Many simulants that mimic Moon soil were terrestrially created according to the chemical and physical characterization of the original lunar samples [2]. For the present research, the test material, simulants LMS-1 and JSC-2A were used in experimental and simulation parts.

Additive Manufacturing (AM) by 3D Printing (3DP), Selective Laser Sintering (SLS) and Selective Laser Melting (SLM) are just a few example of technologies which have given good results in utilization of powder in manufacturing of 3D objects [3]. For that reason, those technologies in combination with lunar raw material will be suited for on-site manufacturing infrastructure on the Moon.

Using in-situ materials and laser technology for construction of the lunar habitats avoids the need to bring significant quantities of resources from the Earth to the Moon.

This paper is introducing the comparative results obtained between simulation done by COMSOL Multiphysics model and from experimental outputs done at ICube laboratory, Illkirch, France. The objective was to create 2D structures by selected laser melting of diverse lunar simulants by optimizing the sintering process though the simulation.

2. MATERIALS AND METHODS

Nano-sized Lunar regolith simulants are materials developed by University of Central Florida (LMS-1) and JSC-2A by NASA.

First things first, information regarding the chemical and physical composition of material has to be known, mainly crystallinity, particles size distribution, shape, and cohesion for the reason to understand its interrelation behavior during the AM procedures [4–7]. Viscosity temperature and wetting behavior are playing important role in parametrization of AM settings [8]. During the heating process, material is passing through several phases to achieve final glassy phase. Geometric shape of melting pool depends on fixed viscosity points and that is where the viscosity temperature and wetting behavior have to be observed and adjust by control of energy intensity and speed.

Behavior of lunar soil in AM process is similar to behavior of metal powder under the same conditions. The norm ISO 7884-2:1987 defines the "workability range" of glassy material which represents the viscosity range between working and Littleton points [9]. Those points are helping to optimize the parameters during the AM process and to better control thermal system. Unfortunately, similar standard for moon dust does not exist but due to similarity between metal powder and lunar simulants this can be applicable until the point when wettability of material starts to affect the consolidation of printed layers due to composition of the lunar soil. Regarding the lunar soil, the analysis of the chemical composition showed that the regolith is predominantly have silica and aluminum oxides but also contains iron, titanium, calcium and magnesium oxides. [1].

The experimental part was done at the ICube

laboratory, Illkirch, France. A RedPower SPI SP-100C continuous wave fiber laser of 100 W with a Gaussian profile, at wavelength of 1090 nm, and with diameter spot of 0.7 mm was used. A Newport motion controller was used for the table displacement in X direction, while the laser power and time exposure were done with LabVIEW software. Displacements in the Y direction were done manually using a micrometer stage installed directly on top of the X stage underneath the laser focusing set up. In this AM procedure only 2D manufacturing was possible.

In parallel a COMSOL Multiphysics model was developed to understand and optimize the experimental process. The multiphysics model was implemented with the thermal conductivity, density, heat capacity and latent heat of fusion of the regolith simulants. The thermal conductivity was based on these two equations [10–12]:

$$K = 0.001561 + 5.426 \cdot 10^{-11} T^3 \quad (1)$$

$$K = 10^{-9.332 + \frac{1.409\ 10^4}{T}} \quad (2)$$

where T is temperature in K. First equation is representing temperature of material before sintering/melting procedure (T < 1500 K) and second one after melting (T > 1500 K).

Stebbins' model [13] was used to model the evolution of density of material with temperature. The heat capacity was calculated over the three temperature ranges: T< 350 K, 350 K < T < 1500 K, and T >1500 K using the respective equations given by Schreiner *et al.* [14]. A latent heat of fusion of 458 kJ/kg was used according to the model developed by Kang *et al.* [15]. Thermal conductivity of 0.82 W/(mK) is used due to model proposed by Langseth, Cremers and Kang [10][11][15]. Due to the high absorption of regolith (80% in our case), the laser beam was modelled as a Gaussian surface heating source on the top surface.

Convective heat transfer and thermal radiations were considered as energy losses on the top surface. Insulation and a temperature fixed to 293 K were used as numerical conditions on the other boundaries. A mesh size of 100 µm, typically 7 times smaller than the laser spot waist, is imposed on the top surface.

3. RESULTS

The first simulation on COMSOL was done in the static mode what is shown in the Fig. *1*. A power of 10 W was fixed, and time exposure of laser was variable from 5 ms to 10 s. The depth propagation of heat is sensitive to the time of the laser exposure. As expected, with increased time exposures, the size of printed spot increases as well.

From the experimental part the task was to observe the behavior of LMS-1 simulant under the different laser powers, from 5 to 20 W in different time exposure from 1 s to 20 s. As can be seen in Fig. 1 and 2, in case of 10 W power and 5 s exposure, the thickness of the melted spot is approximately 1.3 mm. The experimental results were validated by the simulation. It is confirmed that if the power and time are increasing, the size of printed sample increases respectively as represented in Fig. *2*.

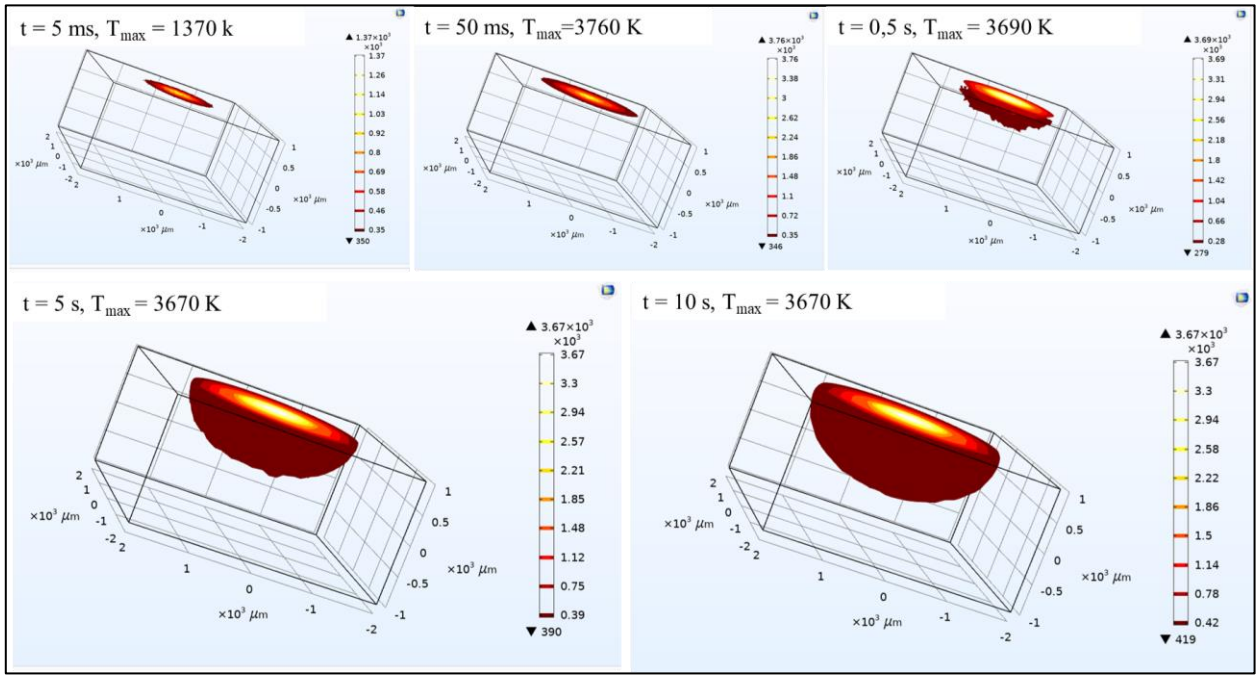

Fig. 1. Simulation of the evolution of the temperature in the static mode for 10 W and spot waist of 700 µm

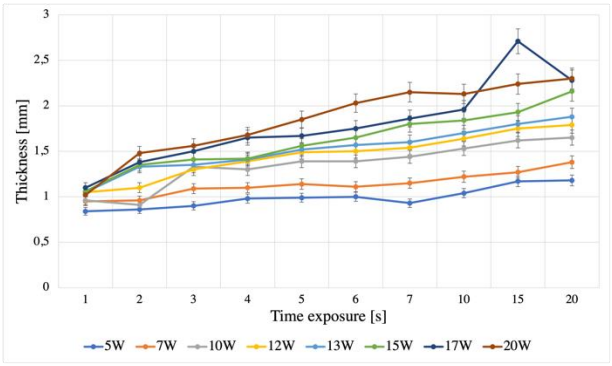

Fig. 2. Experimental results: Thicknesses of melted LMS-1 powder for various time and laser power

Regarding the dynamic mode, the multiphysics model was modified to observe the evolution of temperature when the laser spot is moving. The results displayed in Fig. *3* show the evolution of the melt pool from 10 to 100 ms with power of 25 W, laser speed of 50 mm/s, and spot waist of 700 µm. From this simulation it can be seen that under these conditions, melting of the material happens during all printing process following by cooling coming slowly after. The cooling rate is important to monitor and control when multiple lines will be printed for 2D sample. This parameter has a strong impact on the residual stress and thus the structural integrity of the final printed samples.

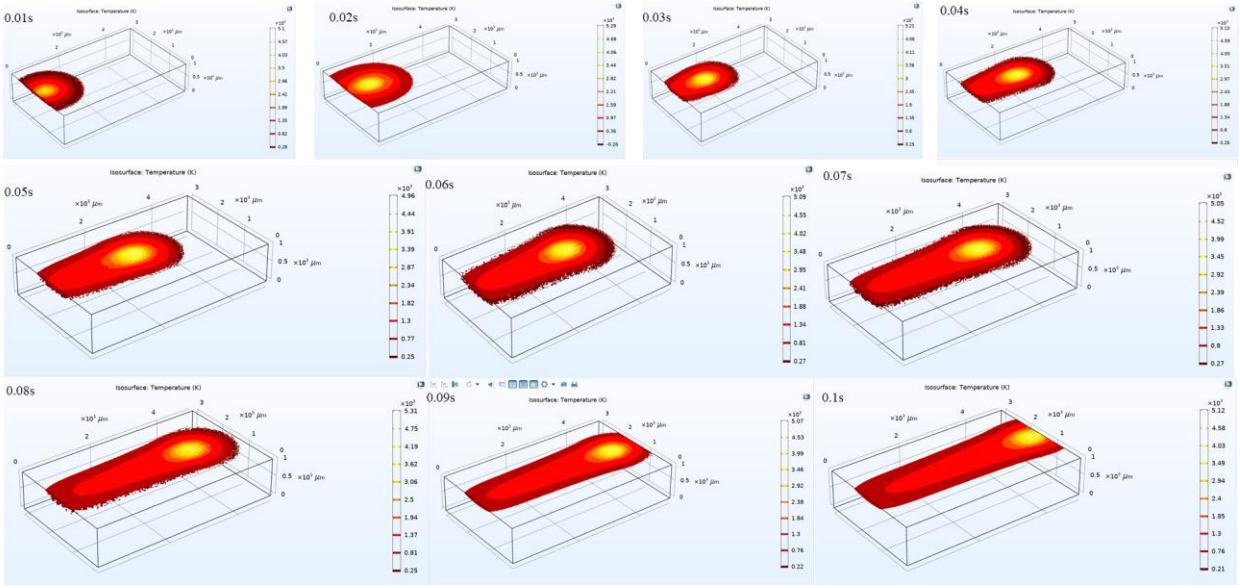

Fig. 3. Thermal analysis in dynamic mode done by COMSOL. 25 W power, laser spot waist of 700 µm, 50 mm/s speed

Fig. 4 shows printed lines of JSC-2A simulant. It can be noticed that when the speed increases, the thickness of the samples is reduced. Likewise, for the same speed, if the power increases, the thickness increases as well.

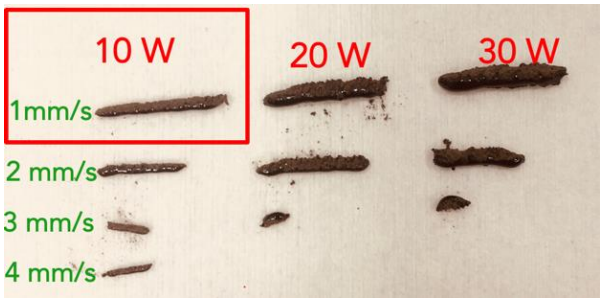

Fig. 4. JSC-2A printed lines under the different laser power and speed with selection of the best suitable combination

The next step in experimental part was to print a square using the best parameters what were applied for previously printed lines. A 10 W laser power and 1 mm/s speed were chosen (see Fig. 4) as a most suitable combination for JSC-2A. The 3D printed square is shown in Fig. *5*. The sample is a 10x10 mm square made of 43 lines with 0.2 mm hatches between lines.

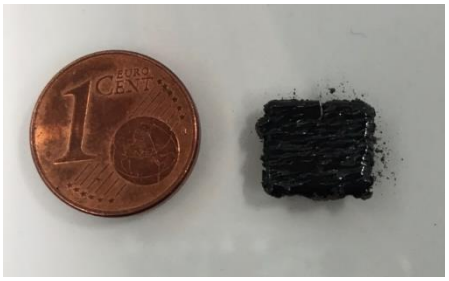

Fig. 5. JSC-2A printed squared

Fig. 6 displays the numerical and experimental results in dynamic mode. The power was varied from 40 to 95 W and speed between 10 and 24 mm/s were used numerically and experimentally. Similar results regarding the thicknesses of the printed samples and melt pool dimensions were found.

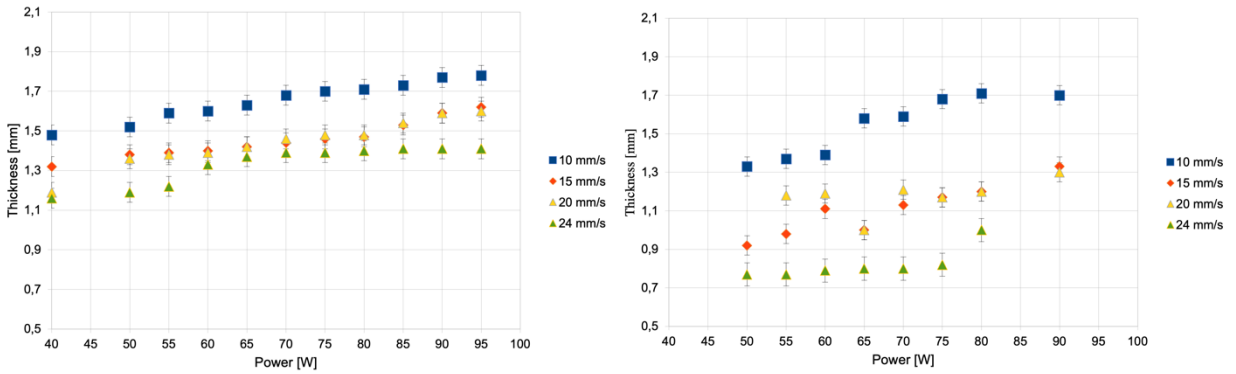

Fig. 6. Comparison between numerical (right) and experimental (left) results

4. DISCUSSION

During the experimental tests it was noticed that laser power, speed of table motion (X direction), distance between printed lines (Y distance) are key parameters that can easily be tailored. The difficulties stand in the control of the energy deposited onto the powder during the processing. The melting and solidification process is governed by the adhesion between the melt pool and the raw material itself. In order to produce continuous lines and avoid the balling effect [16] (due to the surface tension and Marangoni effect), the laser processing parameters has to carefully be selected.

Another care has to be taken to select parameters giving lines with as little residual stress as possible to be able to 3D print surfaces made out of multiple lines. In this case, great care was taken in the optimization of the hatching space between the lines.

During the continuous printing process of a surface, lines one after the other in a raster pattern, the thermally induced mechanical stress and can build up line after line. The final printed simples can therefore present delamination and cracks.

The shape and grain distribution have not been investigated in the study and will surely have a big impact on the quality of the final product [17] Likewise the lack of adequate thermal control of the printed lines (second laser beam to preheat the material or slow down the cooling of the material [18].

Involving a new laser and new material in any sintering experiment, the starting point is to understand the type of interactions under different conditions such as power and speed of table displacement where material is settled.

5. CONCLUSION

There are several parameters which have to be taken into account before sintering procedures start such as the laser parameters, the composition of the raw materials and thus the overall heat transfer mechanism.

Regarding experimental laser tests, interaction of simulant with the laser beam was observed. experimental results are in a good term with COMSOL Multiphysics model. The present results indicate that this methodology of additive manufacturing could be successfully applied to build Lunar habitats.

Further study will include the testing of various powder compactness in a specifically design powder bed and spreader (hopper, blade and roller), test with a galvanic head instead of a stage to reach higher speed, test in a vacuum chamber, the use of other lunar soil simulants and optimization of the multiphysics model.

6. REFERENCES

[1] I.A. Crawford, Lunar resources: A review, Prog. Phys. Geogr. 39 (2015) 137–167. https://doi.org/10.1177/0309133314567585.

[2] L.A. Taylor, C.M. Pieters, D. Britt, Evaluations of lunar regolith simulants, Planet. Space Sci. 126 (2016) 1–7. https://doi.org/10.1016/j.pss.2016.04.005.

[3] M. Fateri, A. Grossmann, S. Fasoulas, A. Großmann, P. Schnauffer, P. Middendorf, Additive Manufacturing of Lunar Regolith for Extra-terrestrial Industry Plant, (2015). https://doi.org/10.1016/j.expneurol.2007.12.026.

[4] L.P. Keller, D.S. McKay, The nature and origin of rims on lunar soil grains, Geochim. Cosmochim. Acta. 61 (1997) 2331–2341. https://doi.org/10.1016/s0016-7037(97)00085-9.

[5] E. Suescun-Florez, S. Roslyakov, M. Iskander, M. Baamer, Geotechnical Properties of BP-1 Lunar Regolith Simulant, J. Aerosp. Eng. 28 (2015) 04014124. https://doi.org/10.1061/(asce)as.1943-5525.0000462.

[6] W.D. Carrier, Particle Size Distribution of Lunar Soil, J. Geotech. Geoenvironmental Eng. 129 (2003) 956–959. https://doi.org/10.1061/(asce)1090-0241(2003)129:10(956).

[7] Y. Li, X. Zeng, A. Wilkinson, Measurement of Small Cohesion of JSC-1A Lunar Simulant, J. Aerosp. Eng. 26 (2013) 882–886. https://doi.org/10.1061/(asce)as.1943-5525.0000197.

[8] M. Fateri, S. Pitikaris, M. Sperl, Investigation on Wetting and Melting Behavior of Lunar Regolith Simulant for Additive Manufacturing Application, Microgravity Sci. Technol. 31 (2019) 161–167. https://doi.org/10.1007/s12217-019-9674-5.

[9] ISO 7884-2:1987 - Glass -- Viscosity and viscometric fixed points, 1987.

[10] M.G.. J. Langseth, S.P.. J. Clark, J.L.. J. Chute, S.J.

Keihm, A.E. Wechsler, Heat flow experiment, NASA. Manned Spacecr. Cent. Apollo 15 Prelim. Sci. Rept. (1972).
[11] C.J. Cremers, Thermophysical properties of Apollo 14 fines, J. Geophys. Res. 80 (1975) 4466–4470. https://doi.org/10.1029/JB080I032P04466.
[12] P. Richet, Y. Bottinga, Thermochemical properties of silicate glasses and liquids: A review, Rev. Geophys. 24 (1986) 1–25. https://doi.org/10.1029/RG024I001P00001.
[13] J.F. Stebbins, I.S.E. Carmichael, L.K. Moret, Heat capacities and entropies of silicate liquids and glasses, Contrib. to Mineral. Petrol. 1984 862. 86 (1984) 131–148. https://doi.org/10.1007/BF00381840.
[14] S.S. Schreiner, J.A. Dominguez, L. Sibille, J.A. Hoffman, Thermophysical property models for lunar regolith, Adv. Sp. Res. 57 (2016) 1209–1222. https://doi.org/10.1016/J.ASR.2015.12.035.
[15] Y. Kang, K. Morita, Thermal conductivity of the CaO-Al_2O_3-SiO_2 system, ISIJ Int. 46 (2006) 420–426.
[16] L. Moniz, Q. Chen, G. Guillemot, M. Bellet, C.A. Gandin, C. Colin, J.D. Bartout, M.H. Berger, Additive manufacturing of an oxide ceramic by laser beam melting—Comparison between finite element simulation and experimental results, J. Mater. Process. Technol. 270 (2019) 106–117. https://doi.org/10.1016/J.JMATPROTEC.2019.02.004.
[17] S. Spath, H. Seitz, Influence of grain size and grain-size distribution on workability of granules with 3D printing, Int. J. Adv. Manuf. Technol. 70 (2014) 135–144. https://doi.org/10.1007/S00170-013-5210-8.
[18] A. MJ, N. DS, P. HS, Investigation of SLM Process in Terms of Temperature Distribution and Melting Pool Size: Modeling and Experimental Approaches, Mater. (Basel, Switzerland). 12 (2019). https://doi.org/10.3390/MA12081272.

Authors: **Danijela Ignjatović Stupar,** International Space University, 1 rue Dominique Cassini, 67400 Illkirch-Graffenstaden, France
E-mail: danijela.stupar@isunet.edu
Grégoire Robert Chabrol, ECAM Strasbourg-Europe Espace Européen de l'Entreprise, 2 Rue de Madrid, 67300 Schiltigheim, France
E-mail: Gregoire.Chabrol@ecam-strasbourg.eu
Abdoul Razak Ibrahim Baraze, Sylvain Lecler, Alexandre Tessier, INSA of Strasbourg -Unistra – CNRS, ICube, 300 bd Sébastien Brant – CS 10413, 67412 Illkirch Cedex, France
E-mail: abdoulrazakbaraze@yahoo.com; sylvain.lecler@insa-strasbourg fr; alexandre.tessier@insa-strasbourg.fr
Thierry Cutard, IMT Mines Albi-Carmaux, École Mines-Télécom, Campus Jarlard, 81013 Albi Ct Cedex 09, France
E-mail: thierry.cutard@mines-albi fr
Jocelyne Brendle, Institut de Science des Matériaux de Mulhouse, UMR CNRS-UHA 7361, 15 rue Jean Stracky, 68057Mulhouse Cedex, France
E-mail: jocelyne.brendle@uha.fr